Journal of Saudi Chemical Society (2017) **21**, S202–S218

King Saud University

Journal of Saudi Chemical Society

www.ksu.edu.sa
www.sciencedirect.com

ORIGINAL ARTICLE

Synthesis, spectroscopic characterization, electrochemistry and biological activity evaluation of some metal (II) complexes with ONO donor ligands containing indole and coumarin moieties

Karekal Mahendra raj, Bennikallu Hire Mathada Mruthyunjayaswamy *

Department of Studies and Research in Chemistry, Gulbarga University, Gulbarga 585 106, Karnataka, India

Received 27 September 2013; revised 19 December 2013; accepted 8 January 2014
Available online 23 January 2014

KEYWORDS

Indole;
Coumarin;
Thermogravimetry–differential thermal analysis;
Electrochemistry;
Antimicrobial and antioxidant activity

Abstract Cu(II), Co(II), Ni(II) and Zn(II) complexes of ligands 5-substituted-*N*′-((7-hydroxy-4-methyl-2-oxo-2*H*-chromen-8-yl)methylene)-3-phenyl-1*H*-indole-2-carbohydrazides were synthesized, characterized by elemental analysis and various spectroscopic techniques like, IR, ^{1}H NMR, ESI-mass, UV–Visible, thermogravimetry–differential thermal analysis, magnetic measurements, molar conductance and powder-XRD data. Spectral analysis indicates octahedral geometry for all the complexes. Cu(II) and Zn(II) complexes of both the ligands have 1:1 stoichiometry of the type $[M(L)(Cl)(H_2O)_2]$, whereas Co(II) and Ni(II) complexes of both the ligands have 1:2 stoichiometric ratio of the type $[M(L)_2]$. The bonding sites are the oxygen atom of amide carbonyl, nitrogen of azomethine function and phenolic oxygen for the Schiff base ligands. The thermogravimetry–differential thermal analysis studies gave evidence for the presence of coordinated water molecules in the composition of Cu(II) and Zn(II) complexes of both the ligands, which were further supported by IR measurements. All the complexes were investigated for their electrochemical activity, but only the Cu(II) complexes showed the redox property. In order to evaluate the effect of antimicrobial potency of metal ions upon chelation, ligands and their metal complexes along with their respective metal chlorides were screened for their antibacterial and antifungal activities by the minimum inhibitory concentration (MIC) method. The results showed that the metal complexes were found to be more active than free ligands. Ligand **1** and its complexes were screened for free radical scavenging activity by the DPPH method and DNA cleavage activity using supercoiled plasmid DNA.

* Corresponding author. Tel.: +91 9448830318.
E-mail address: bhmmswamy53@rediffmail.com (B.H.M. Mruthyunjayaswamy).
Peer review under responsibility of King Saud University.

Production and hosting by Elsevier

1. Introduction

Metal coordination compounds as therapeutics for cancer, malaria and other medicinal applications have been investigated [1-3]. Platinum complexes, such as cisplatin, carboplatin and oxaliplatin represent the most successful drugs against

http://dx.doi.org/10.1016/j.jscs.2014.01.001
1319-6103

specific cancer types. Many transition metal complexes with copper [4], cobalt [5], iron [6] and vanadium [7] have been reported as efficient DNA cleavage agents with or without sequence specificity, moreover the ligand or the metal in these complexes can be varied in an easily controlled manner to facilitate the individual applications [8].

Indole is the parent substance of a large number of important compounds and also it is one of the most abundant and relevant heterocycles in natural products and pharmaceuticals. Therefore, indole plays an important role in the synthesis of new pharmaceutical products. A large number of pharmacodynamic compounds containing indole moiety have been reported to possess a several biological properties *viz*. antibacterial [9], anti-inflammatory [10,11], anticonvulsant [12], antiviral [13], cardiovascular [14] and COX-2 inhibitor activities [15,16]. More specifically, several reports describe that indole-2-carbohydrazides and related compounds are endowed with MAO inhibitory [17], antihistaminic [18] and antidepressant activities [19]. Complexing reactions of indole derivatives with bio metals resulted in the compounds which are used to treat diseases like depression, rheumatism, migraine and some types of cancer [20].

Coumarin (2*H*-chromen-2-one) and its derivatives consisting of fused benzene and α-pyrone rings are widely distributed in nature and exhibit a broad pharmacological profile [21]. Coumarin analogs are considered to be important class of compounds due to their several applications in the medical fields [22-24]. Interest in coumarin derivatives is rapidly increasing in connection with the marked biological implication of coumarins particularly in the treatment of human immunodeficiency virus, because of their ability to inhibit human immunodeficiency virus integrase [25,26]. Synthesis of coumarins and their derivatives have attracted much attention of medicinal and organic chemists, as they are widely used in pharmaceuticals, fragrances, agrochemicals, food additives, optical brightener and laser dyes [27,28]. A large number of coumarin derivatives were found to possess tissue protective antioxidant properties by affecting the formation and scavenging of reactive nitrogen species (RNS) and scavenging of reactive oxygen species (ROS) [29]. Among them, hydroxyl substituted coumarins act as effective metal chelators, free radical scavengers and powerful chain breaking antioxidants. Nowadays, antioxidant activates gained much interest, particularly in preventing the adverse effects caused by the free radicals in the human body are attracting ones. The free radicals are also associated with arthritis, inflammation, diabetes, carcinogenesis, mutagenesis and genotoxicity due to the oxidative stress which arises due to imbalance between free radical generations [30]. Antioxidant activity of metal complex is found to be induced by both the identity of the metal and the ligands bound to it [31]. In view of these findings and in continuation of our work on coordination chemistry [32–38], we found it is worth to synthesize Schiff base ligands containing both indole and coumarin moieties *viz*. 5-substituted-*N*′-((7-hydroxy-4-methyl-2-oxo-2*H*-chromen-8-yl)methylene)-3-phenyl-1*H*-indole-2-carbohydrazide and their metal complexes and to study their pharmacological activities like antimicrobial, antioxidant and DNA cleavage activities.

2. Experimental

2.1. Analysis and physical measurements

IR spectra of the ligands and metal complexes were recorded as KBr pellets on a Perkin Elmer – Spectrum RX-IFTIR instrument covering the range 4000–250 cm^{-1}. Elemental analysis was obtained from a Perkin Elmer 2400 CHN Elemental Analyzer which is a microprocessor based instrument. ^{1}H NMR spectra of ligands and their Zn(II) complexes were recorded on the FT NMR Spectrometer model Avance-II (Bruker), 400 MHz instrument using d_6-DMSO as solvent. ESI-MS was recorded on a mass spectrometer equipped with electrospray ionization (ESI) and atmospheric pressure chemical ionization (APCI) sources having mass range of 4000 amu in quadruple and 20,000 amu in ToF. UV–Visible spectra of the Cu(II), Co(II) and Ni(II) complexes were recorded on a Elico – SL 164 double beam UV–Visible spectrophotometer in the range 200–1000 nm in dimethyformamide (DMF) solution (1×10^{-3} M). At room temperature ESR spectra of the Cu(II) complexes in the polycrystalline state were recorded on a BRUKER Bio Spin Gmbh spectrometer at a microwave frequency of 9.1 GHz. The experiment was carried out by using DPPH as reference with field set at 3000 gauss using tetracynoethylene as the 'g' marker (g = 2.00277). Powder-XRD of the complexes was recorded using a Bruker AXS D8 Advance (Cu, Wavelength 1.5406 Å source). Electrochemistry of all the complexes was recorded on a 600 D series model electrochemical analyzer in DMF using tetrabutylammonium perchlorate as a supporting electrolyte. Molar conductivity measurements were recorded on an ELICO CM-180 conductivity bridge in dry DMF (10^{-3} M) solution using a dip-type conductivity cell fitted with a platinum electrode and the magnetic susceptibility measurements were made at room temperature on a Gouy balance using $Hg[Co(NCS)_4]$ as the calibrant.

2.2. Methods

All the chemicals used were of high purity grade; solvents were dried and distilled before use. Melting points of the ligands and their complexes were determined by electro-thermal apparatus using open capillary tubes. The metal and chloride contents were determined as per standard procedures [39]. The precursors 5-substituted-3-phenyl-1*H*-indole-2-carboxyhydrazide and 8-formyl-7-hydroxy-4-methylcoumarin were prepared by the literature methods [40,41].

2.3. Synthesis of the ligands *1* and *2*

Equimolar mixture of 5-substituted-3-phenyl-1*H*-indole-2-carboxyhydrazide (0.001 mol) and 8-formyl-7-hydroxy-4-methylcoumarin (0.001 mol) with 1–2 drops of glacial acetic acid as a catalyst in methanol (20 mL) was refluxed on a water bath for about 4–5 h. The reaction was monitored by TLC. The yellow solid separated was filtered, washed with hot methanol, dried and recrystallized from dioxane (Scheme 1).

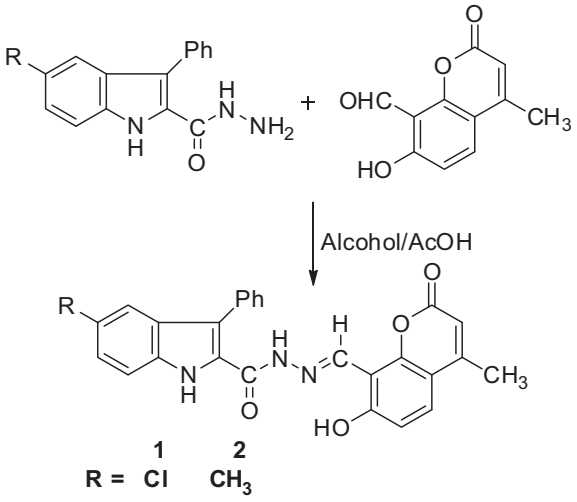

Scheme 1 Synthesis of ligands **1** and **2**.

*2.3.1. Ligand **1***

Yield = 71%. m.p. 298 °C; Anal. Calcd. (%) for $C_{26}H_{18}N_3O_4Cl$: (Mol. Wt. = 471 g) C, 66.24; H, 3.82; N, 8.91; Cl, 7.43. Found (%): C, 66.32; H, 3.91; N, 9.01; Cl, 7.32. FT-IR (KBr, cm^{-1}): 3418 br, *v*(OH); 3240 *v*(indole-NH); 3057, *v*(amide-NH); 1720, *v*(lactone C═O); 1677, *v*(amide C═O); 1612, *v*(C═N); 1230, *v*(C–O). ^{1}H NMR (d_6-DMSO, ppm): 12.62 (s, 1H, phenolic OH); 12.18 (s, 1H, CONH); 12.04 (s, 1H, indole-NH); 8.85 (s, 1H, HC═N); 7.31–7.72 (m, 10H, ArH); 6.24 (s, 1H, vinyl CH); 2.40 (s, 3H, coumarin CH_3). ESI-MS ($_M^{\bullet}$, $_M^{\bullet}$ +2): 471, 473 (100%, 30%).

*2.3.2. Ligand **2***

Yield = 67%; m.p. 287 °C; Anal. Calcd. (%) for $C_{27}H_{21}N_3O_4$: (Mol. Wt. = 451 g) C, 71.84; H, 4.65; N, 9.31. Found (%): C, 71.72; H, 4.77; N, 9.47. FT-IR (KBr, cm^{-1}): 3460 br, *v*(OH); 3245 *v*(indole-NH); 3052, *v*(amide-NH); 1713, *v*(lactone C═O); 1673, *v*(amide C═O); 1614, *v*(C═N); 1232, *v*(C–O). ^{1}H NMR (d_6-DMSO, ppm): 12.68 (s, 1H, phenolic OH); 11.93 (s, 1H, CONH); 11.80 (s, 1H, indole-NH); 8.86 (s, 1H, HC═N); 6.96–7.40 (m, 10H, ArH); 6.25 (s, 1H, vinyl CH); 2.40 (s, 3H, coumarin CH_3); 2.39 (s, 3H, indole-CH_3). ESI-MS ($_M^{\bullet}$): 451 (100%).

*2.4. Preparation of Cu(II), Co(II), Ni(II) and Zn(II)complexes of ligands **1** and **2***

To the hot solution of 5-substituted-*N'*-((7-hydroxy-4-methyl-2-oxo-2*H*-chromen-8-yl)methylene)-3-phenyl-1*H*-indole-2-carbohydrazide (0.002 mol) in methanol (30 mL) was added a hot methanolic solution (15 mL) of respective metal chlorides (0.002 mol). The reaction mixture was refluxed on water bath for about 4 h. Sodium acetate (0.5 g) was added to the reaction mixture to maintain a neutral pH and refluxing was continued for 1 h more. The reaction mixture was poured into distilled water. The colored solid complexes separated were collected by filtration, washed with sufficient quantity of distilled water, then with hot methanol to apparent dryness and dried in a vacuum over anhydrous calcium chloride in a desiccator. The melting points of all the compounds are depicted in Table 1.

*2.4.1. Cu(II) complex (**1a**)*

Yield = 68%. m.p. >300 °C; Anal. Calcd. (%) for [Cu($C_{26}H_{17}N_3O_4Cl$)(Cl)(H_2O)$_2$]: (Mol. Wt. = 604.54 g) C, 51.60; H, 3.47; N, 6.94; Cl, 11.57; Cu, 10.51. Found (%): C, 51.74; H, 3.56; N, 7.08; Cl, 11.41; Cu, 10.43. FT-IR (KBr, cm^{-1}): 3411 br, *v*(H_2O); 3249, *v*(indole-NH); 3056, *v*(amide NH); 1723, *v*(lactone C═O); 1628, *v*(amide C═O); 1561, *v*(HC═N); 1289, *v*(C–O); 542, *v*(M–O); 473, *v*(M–N); 326, *v*(M–Cl). ESI-MS ($_M^{\bullet}$ + 1, $_M^{\bullet}$ + 2): 605, 607 (10%, 2.7%). UV–Vis (DMF): 13,590–17,876 cm^{-1}.

*2.4.2. Co(II) complex (**1b**)*

Yield = 59%. m.p. >300 °C; Anal. Calcd. (%) for [Co($C_{26}H_{17}N_3O_4Cl$)$_2$]: (Mol. Wt. = 998.93 g) C, 62.46; H, 3.40; N, 8.40; Cl, 7.00; Co, 5.89. Found (%): C, 62.38; H, 3.55; N, 8.59; Cl, 6.91; Co, 5.94. FT-IR (KBr, cm^{-1}): 3246, *v*(indole-NH); 3053, *v*(amide-NH); 1719, *v*(lactone C═O); 1619, *v*(amide C═O); 1580, *v*(HC═N); 1293, *v*(C–O); 529, *v*(M–O); 478, *v*(M–N). ESI-MS ($_M^{\bullet}$, $_M^{\bullet}$ + 2): 998, 1000 (12%, 4.5%). UV–Vis (DMF): v_1, 7912 cm^{-1}; v_2, 16,982; v_3, 21,237 cm^{-1}.

*2.4.3. Ni(II) complex (**1c**)*

Yield = 56%. m.p. >300 °C; Anal. Calcd. (%) for [Ni($C_{26}H_{17}N_3O_4Cl$)$_2$]: (Mol. Wt. = 998.69 g) C, 62.48; H, 3.40; N, 8.41; Cl, 7.00; Ni, 5.87. Found (%): C, 62.59; H, 3.56; N, 8.30; Cl, 7.14; Ni, 5.69. FT-IR (KBr, cm^{-1}): 3245, *v*(indole-NH); 3076, *v*(amide-NH); 1717, *v*(lactone C═O); 1617, *v*(amide C═O); 1580, *v*(HC═N); 1293, *v*(C–O); 534, *v*(M–O); 493, *v*(M–N). UV–Vis (DMF): v_1, 8210 cm^{-1}; v_2, 13,598; v_3, 23,874 cm^{-1}.

*2.4.4. Zn(II) complex (**1d**)*

Yield = 66%. m.p. >300 °C; Anal. Calcd. (%) for [Zn($C_{26}H_{17}N_3O_4Cl$)(Cl)(H_2O)$_2$]: (Mol. Wt. = 606.40 g) C, 51.45; H, 3.46; N, 6.92; Cl, 11.54; Zn, 10.78. Found (%): C, 51.59; H, 3.57; N, 7.08; Cl, 11.40; Zn, 10.63. FT-IR (KBr, cm^{-1}): 3411 br, *v*(H_2O); 3247, *v*(indole-NH); 3057, *v*(amide NH); 1718, *v*(lactone C═O); 1614, *v*(amide C═O); 1578, *v*(HC═N); 1291, *v*(C–O); 509, *v*(M–O); 455, *v*(M–N); 366, *v*(M–Cl). ^{1}H NMR (d_6-DMSO, ppm): 12.27 (s, 1H, CONH); 12.05 (s, 1H, indole-NH); 8.87 (s, 1H, HC═N); 7.33–7.74 (m, 10H, ArH); 6.46 (s, 1H, vinyl CH); 2.40 (s, 3H, coumarin CH_3). ESI-MS ($_M^{\bullet}$ + 1, $_M^{\bullet}$ + 2): 607, 609 (13%, 3.2%).

*2.4.5. Cu(II) complex (**2a**)*

Yield = 65%. m.p. >300 °C; Anal. Calcd. (%) for [Cu($C_{27}H_{20}N_3O_4$)(Cl)(H_2O)$_2$]: (Mol. Wt. = 584.54 g) C, 55.42; H, 4.10; N, 7.18; Cl, 5.98; Cu, 10.87. Found (%): C, 55.59; H, 4.23; N, 7.25; Cl, 5.90; Cu, 10.74. FT-IR (KBr, cm^{-1}): 3388 br, *v*(H_2O); 3247, *v*(indole-NH); 3051, *v*(amide-NH); 1718, *v*(lactone C═O); 1621, *v*(amide C═O); 1547, *v*(HC═N); 1279, *v*(C–O); 566, *v*(M–O); 460, *v*(M–N); 333, *v*(M–Cl). UV–Vis (DMF): 13,782–17,563 cm^{-1}.

*2.4.6. Co(II) complex (**2b**)*

Yield = 54%. m.p. >300 °C; Anal. Calcd. (%) for [Co($C_{27}H_{20}N_3O_4$)$_2$]: (Mol. Wt. = 958.93 g) C, 67.57; H, 4.17; N, 8.75; Co, 6.14. Found (%): C, 67. 71; H, 4.28; N, 8.89; Co, 6.09. FT-IR (KBr, cm^{-1}): 3236, *v*(indole-NH); 3049, *v*(amide

Table 1 Physical, analytical and magnetic susceptibility data of ligands **1** and **2** and their complexes.

Ligand/complexes	Molecular formula	Mol. Wt. (g)	M.p. °C (yield %)	Elemental analysis (%) Calcd (Found)					Mag. Moment μeff (BM)	Molar conductance (μ_M) ohm^{-1} cm^2 mol^{-1}	Color
				M	C	H	N	Cl			
1 HL_1	$C_{26}H_{18}N_3O_4Cl$	471	298 (71)	–	66.24 (66.32)	3.82 (3.91)	8.91 (9.01)	7.43 (7.32)	–	–	Yellow
2 HL_2	$C_{27}H_{21}N_3O_4$	451	287 (67)	–	71.84 (71.72)	4.65 (4.77)	9.31 (9.47)	–	–	–	Yellow
1a $[Cu(L_1)(Cl)(H_2O)_2]$	$[Cu(C_{26}H_{17}N_3O_4Cl)(Cl)(H_2O)_2]$	604.54	> 300 (68)	10.51 (10.43)	51.60 (51.74)	3.47 (3.56)	6.94 (7.08)	11.57 (11.41)	1.79	31	Green
1b $[Co(L_1)_2]$	$[Co(C_{26}H_{17}N_3O_4Cl)_2]$	998.93	> 300 (59)	5.89 (5.94)	62.46 (62.38)	3.40 (3.55)	8.40 (8.59)	7.00 (6.91)	5.01	19	Brown
1c $[Ni(L_1)_2]$	$[Ni(C_{26}H_{17}N_3O_4Cl)_2]$	998.69	> 300 (56)	5.87 (5.69)	62.48 (62.59)	3.40 (3.56)	8.41 (8.30)	7.00 (7.14)	2.90	20	Green
1d $[Zn(L_1)(Cl)(H_2O)_2]$	$[Zn(C_{26}H_{17}N_3O_4Cl)(Cl)(H_2O)_2]$	606.40	> 300 (66)	10.78 (10.63)	51.45 (51.59)	3.46 (3.57)	6.92 (7.08)	11.54 (11.40)	–	30	Orange
2a $[Cu(L_2)(Cl)(H_2O)_2]$	$[Cu(C_{27}H_{20}N_3O_4)(Cl)(H_2O)_2]$	584.54	> 300 (65)	10.87 (10.74)	55.42 (55.59)	4.10 (4.23)	7.18 (7.25)	5.98 (5.90)	1.80	28	Green
2b $[Co(L_2)_2]$	$[Co(C_{27}H_{20}N_3O_4)_2]$	958.93	> 300 (54)	6.14 (6.09)	67.57 (67.71)	4.17 (4.28)	8.75 (8.89)	–	5.12	16	Brown
2c $[Ni(L_2)_2]$	$[Ni(C_{27}H_{20}N_3O_4)_2]$	958.69	> 300 (57)	6.12 (6.02)	67.59 (67.42)	4.17 (4.29)	8.76 (8.84)	–	2.97	18	Green
2d $[Zn(L_2)(Cl)(H_2O)_2]$	$[Zn(C_{27}H_{20}N_3O_4)(Cl)(H_2O)_2]$	586.40	> 300 (61)	11.15 (11.02)	55.25 (55.33)	4.09 (4.17)	7.16 (7.20)	5.96 (5.84)	–	26	Orange

NH); 1712, *ν*(lactone C═O); 1615, *ν*(amide C═O); 1577, *ν*(HC═N); 1287, *ν*(C–O); 536, *ν*(M–O); 468, *ν*(M–N). UV–Vis (DMF): ν_1, 7504 cm^{-1}; ν_2, 16,114; ν_3, 20,385 cm^{-1}.

2.4.7. Ni(II) complex (**2c**)

Yield = 57%. m.p. >300 °C; Anal. Calcd. (%) for [Ni($C_{27}H_{20}N_3O_4)_2$]: (Mol. Wt. = 958.69 g) C, 67.59; H, 4.17; N, 8.76; Ni, 6.12. Found (%): C, 67. 42; H, 4.29; N, 8.84; Ni, 6.02. FT-IR (KBr, cm^{-1}): 3248, *ν*(indole-NH); 3049, *ν*(amide NH); 1716, *ν*(lactone C═O); 1611, *ν*(amide C═O); 1578, *ν*(HC═N); 1299, *ν*(C–O); 550, *ν*(M–O); 478, *ν*(M–N). UV–Vis (DMF): ν_1, 8410 cm^{-1}; ν_2, 13,894; ν_3, 24,194 cm^{-1}.

2.4.8. Zn(II) complex (**2d**)

Yield = 61%. m.p. >300 °C; Anal. Calcd. (%) for [Zn($C_{27}H_{20}N_3O_4$)(Cl)(H_2O)$_2$]: (Mol. Wt. = 586.40 g) C, 55.25; H, 4.09; N, 7.16; Cl, 5.96; Zn, 11.15. Found (%): C, 55.33; H, 4.17; N, 7.20; Cl, 5.84; Zn, 11.02. FT-IR (KBr, cm^{-1}): 3435 br, *ν*(H_2O); 3254, *ν*(indole-NH); 3053, *ν*(amide NH); 1712, *ν*(lactone C═O); 1618, *ν*(amide C═O); 1577, *ν*(HC═N); 1298, *ν*(C–O); 570, *ν*(M–O); 466, *ν*(M–N); 366, *ν*(M–Cl). ^{1}H NMR (d_6-DMSO, ppm): 12.11 (s, 1H, CONH); 11.89 (s, 1H, indole-NH); 8.95 (s, 1H, HC═N); 6.98–7.61 (m, 10H, ArH); 6.40 (s, 1H, vinyl CH); 2.53 (s, 3H, coumarin CH_3); 2.40 (s, 3H, indole CH_3).

2.5. Pharmacology

2.5.1. Antimicrobial assays

The synthesized Schiff bases **1** and **2** and their metal complexes were studied for their antibacterial and antifungal activities by the Muller-Hinton agar (MHA) and potato dextrose agar (PDA) dilution method respectively. The *in vitro* antibacterial activities of the test compounds were tested against two Gram-positive *Bacillus subtilis* (MTCC 736) and *Staphylococcus aureus* (MTCC 3160) and two Gram-negative *Escherichia coli* (MTCC 46) and *Salmonella typhi* (MTCC 98) bacteria. The *in vitro* antifungal activities were carried out against *Aspergillus niger* (MTCC 1881), *Cladosporium oxysporum* (MTCC 1777) and *Candida albicans* (MTCC 227) fungi in accordance with the international recommendation provided by the Clinical and Laboratory Standard Institute (CLSI). The stock solutions of the each test compound and their respective metal chlorides (1 mg mL^{-1}) were prepared by dissolving 10 mg of the each sample in 10 mL of freshly distilled DMSO solvent. Further, the different concentrations of the test samples (100, 75, 50, 25 and 12.5 μg mL^{-1}), were prepared by diluting the stock solution with the required amount of freshly distilled DMSO.

For antibacterial activity, Muller-Hinton agar plates containing final concentration of 100, 75, 50, 25 and 12.5 μg mL^{-1} of each test compound and their respective metal chlorides were inoculated with standardized inoculum of test strains of bacteria (McFarland standard 0.5). Before inoculation these plates were incubated overnight to check the purity. Using the standard multipoint inoculator, test bacterial culture was inoculated on the surface of the Muller-Hinton agar and the plates were kept for incubation at 37 °C in inverted position. One control plate of Muller-Hinton agar without the test compound was incubated with test strains of bacteria and kept for incubation at the same condition. After 24 h of incubation MIC (minimal inhibitory concentration) of each test compound was recorded as the lowest concentration of compound with no visible growth of bacteria.

For antifungal activity, potato dextrose agar plates containing final concentration of 100, 75, 50, 25 and 12.5 μg mL^{-1} of each test compound and their respective metal chlorides were inoculated with 100 μL of spore suspension of 7 day old culture of test fungi (10^8 spore/ml). These plates were kept for incubation at 32 °C. Along with these plates one control plate without test compound was inoculated with its respective test strains of fungi and was placed for incubation at the above described condition. After 48 h of incubation MIC (minimal inhibitory concentration) of each test compound was recorded as the lowest concentration of compound with no visible growth of fungi.

The minimum concentration of each test compound with no visible growth of test bacteria/fungi was reported as MIC for their respective strains. Blank tests have shown that DMSO in the preparation of the test solution does not affect the test organisms. The results were compared with that of gentamycin, a broad-spectrum antibiotic for bacterial strains and fluconazole for fungal strains as positive control.

2.5.2. Antioxidant assay (free radical scavenging activity)

The free radical scavenging activity of ligand and its metal complexes were determined with the 2,2-diphenyl-1-picrylhydrazyl (DPPH) method [42]. Different concentrations of compounds (12.5, 25, 50 and 100 μg) and standard butylated hydroxy anisole (BHA) were taken in different test tubes. The volume of each test tube was adjusted to 100 μL by adding distilled DMF. To each test solution in DMF, 5 mL methanolic solution of DPPH (0.1 mM) was added to these tubes. The tubes were kept at ambient temperature for 30 min. The control experiment was carried out as above without the test samples. The absorbance of test solutions was measured at 517 nm. The decrease in the absorbance of DPPH was calculated comparative to the measured absorbance of the control. The percentage radical scavenging activity was calculated using the following formula:

$$\%\ \text{Radical scavenging activity} = \left[\frac{\text{Control optical density} - \text{Sample optical density}}{\text{Control optical density}}\right] \times 100$$

2.5.3. DNA cleavage experiment

The extent to which the synthesized compounds could serve as DNA cleavage agents was studied using supercoiled plasmid DNA pBR 322 (Bangal re Genei, Bengaluru, Cat. No. 105850) as a target molecule. The agarose gel electrophoresis method was employed to test the efficiency of cleavage by the synthesized compounds. Each test compound (100 μg) was added separately to the 225 ng pBR 322 DNA sample and these samples mixtures were incubated at 37 °C for 2 h. The electrophoresis of the test compounds was done according to the literature method [43]. Mixture of agarose (600 mg) and hot tris–acetate-EDTA (TAE) buffer (60 mL) (4.84 g Tris base, pH-8.0, 0.5 M EDTA L^{-1}) was heated to boil for few minutes. The hot gel was poured into the gas cassette fitted with comb. On cooling to room temperature gel gets solidified and the solidified gel was placed in the electrophoresis chamber containing TAE buffer. Equimolar mixture DNA sample

(20 μL) initially treated with the test compounds and bromophenol blue dye along with standard DNA marker containing TAE buffer was loaded carefully into the wells and a constant electricity of 50 V was supplied for about 40 min. Later, the gel was removed and it is stained with ethidium bromide solution (10 μg mL^{-1}) for 10–15 min and the bands were observed and photographed under UV-illuminator.

3. Results and discussion

All the synthesized metal complexes are colored solids, amorphous and non-hygroscopic in nature and possess high melting points (> 300 °C). The complexes are insoluble in water and common organic solvents but are soluble in DMF and DMSO. Elemental analysis and analytical data of the complexes suggest that the metal to ligand ratio of the complexes is 1:1 stoichiometry of the type $[M(L)(Cl)(H_2O)_2]$ for Cu(II) and Zn(II) complexes and 1:2 stoichiometry of the type $[M(L)_2)]$ for Co(II) and Ni(II) complexes of ligands **1** and **2** respectively, where L stands for deprotonated ligand. The molar conductance values are too low to account for any dissociation of the complexes in DMF (16–31 ohm^{-1} cm^2 $mole^{-1}$), indicating their non-electrolytic nature (Table 1) [44].

3.1. IR spectral studies

The important IR bands of the ligands and their metal complexes are represented in Table 2. In the IR spectra of ligands **1** and **2**, absorption due to phenolic OH have exhibited bands at 3418 and 3460 cm^{-1}, absorption due to indole NH and CONH functions have displayed bands at 3240 and 3057 cm^{-1} and 3245 and 3052 cm^{-1}, respectively. Two sharp peaks observed at 1720 and 1677 cm^{-1} and 1713 and 1673 cm^{-1} are due to the lactone carbonyl function and amide carbonyl function attached to 2-position of indole moiety of both the ligands. Absorption bands due to azomethine function and phenolic C–O function of the ligands **1** and **2** have appeared at 1612 and 1230 cm^{-1} and 1614 and 1232 cm^{-1}, respectively.

The absence of absorption bands due to phenolic OH groups at 3418 and 3460 cm^{-1} in the IR spectra of Cu(II), Co(II), Ni(II) and Zn(II) complexes of ligands **1** and **2** indicates the formation of bonds between metal ion and phenolic oxygen atom *via* deprotonation. This is further confirmed by the increase in absorption frequency of phenolic C–O which appeared in the region 1289–1293 and 1279–1299 cm^{-1}, respectively in the metal complexes of ligands **1** and **2** under the present study. The absorption band due to indole NH and NH of CONH functions of the above metal complexes of ligands **1** and **2** has displayed bands in the region 3245–3249 cm^{-1} and 3053–3076 cm^{-1} and 3236–3254 cm^{-1} and 3049–3053 cm^{-1}, respectively, which have appeared at about the same region as in the case of respective ligands, thus confirming the non-involvement of either indole NH or NH of CONH function in coordination with the metal ions. The absorption band due to lactone carbonyl function in all the metal complexes have appeared at about the same region 1723–1717 and 1718–1712 cm^{-1} of both the ligands **1** and **2**, there by indicating the non-involvement of lactone carbonyl oxygen in coordination with metal ions. The absorption frequency of amide carbonyl and azomethine functions which

Table 2 IR spectral data (cm^{-1}) of ligands **1** and **2** and their complexes.

Ligands/complexes		ν_{H2O}	ν_{OH} (phenolic)	ν_{NH} (indole)	ν_{NH} (amide)	$\nu_{C=O}$ (lactone)	$\nu_{C=O}$ (carbonyl)	$\nu_{C=N}$ (azomethine)	ν_{C-O} (phenolic)	ν_{M-O}	ν_{M-N}	ν_{M-Cl}
1	HL_1	–	3418	3240	3057	1720	1677	1612	1230	–	–	–
2	HL_2	–	3460	3245	3052	1713	1673	1614	1232	–	–	–
1a	$[Cu(L_1)(Cl)(H_2O)_2]$	3411	–	3249	3056	1723	1628	1561	1289	542	473	326
1b	$[Co(L_1)_2]$	–	–	3246	3053	1719	1619	1580	1293	529	478	–
1c	$[Ni(L_1)_2]$	–	–	3245	3076	1717	1617	1580	1293	534	493	–
1d	$[Zn(L_1)(Cl)(H_2O)_2]$	3411	–	3247	3057	1718	1614	1578	1291	509	455	366
2a	$[Cu(L_2)(Cl)(H_2O)_2]$	3388	–	3247	3091	1718	1621	1547	1279	566	460	333
2b	$[Co(L_2)_2]$	–	–	3236	3049	1712	1615	1577	1287	536	468	–
2c	$[Ni(L_2)_2]$	–	–	3248	3049	1716	1611	1578	1299	550	478	–
2d	$[Zn(L_2)(Cl)(H_2O)_2]$	3435	–	3254	3053	1712	1618	1577	1298	570	466	366

Table 3 ^{1}H NMR data of ligands **1** and **2** and their Zn(II) complexes.

Ligands/Zn(II) complexes	^{1}H NMR data (ppm)
1/HL_1	12.62 (s, 1H, phenolic OH), 12.18 (s, 1H, CONH), 12.04 (s, 1H, indole NH), 8.85 (s, 1H, HC═N), 7.31–7.72 (m, 10H, ArH), 6.24 (s, 1H, =CH) and 2.40 (s, 3H, coumarin CH_3)
2/HL_2	12.68 (s, 1H, phenolic OH), 11.93 (s, 1H, CONH), 11.80 (s, 1H, indole NH), 8.86 (s, 1H, HC═N), 6.96–7.40 (m, 10H, ArH), 6.25 (s, 1H, =CH), 2.40 (s, 3H, coumarin CH_3) and 2.39 (s, 3H, indole CH_3)
1d/$[Zn(L_1)(Cl)(H_2O)_2]$	12.27 (s, 1H, CONH), 12.05 (s, 1H, indole NH), 8.87 (s, 1H, HC═N), 7.33–7.74 (m, 10H, ArH), 6.46 (s, 1H, =CH) and 2.40 (s, 3H, coumarin CH_3)
2d/$[Zn(L_2)(Cl)(H_2O)_2]$	12.11 (s, 1H, CONH), 11.89 (s, 1H, indole NH), 8.95 (s, 1H, HC═N), 6.98–7.61 (m, 10H, ArH), 6.40 (s, 1H, =CH), 2.53 (s, 3H, coumarin CH_3) and 2.40 (s, 3H, indole CH_3)

appeared at 1677 and 1612 cm^{-1} and 1673 and 1614 cm^{-1} in case of ligands **1** and **2**, has been shifted to lower frequency by 63–49 and 51–32 cm^{-1} and 62–52 and 67–36 cm^{-1}, respectively in the complexes and appeared in the region 1628–1614 and 1580–1561 cm^{-1} and 1621–1611 and 1578–1547 cm^{-1} indicating the involvement of oxygen atom of carbonyl function as such without undergoing any enolization [45] and nitrogen atom of azomethine [46] function in complexation with the metal ions. This is further confirmed by the appearance of new bands in the region 542–509 and 493–455 cm^{-1} and 570–536 and 478–460 cm^{-1} due to M–O and M–N stretching vibrations [47] in all the complexes of ligands **1** and **2**. The appearance of new bands in the region 366–326 and 366–333 cm^{-1} in Cu(II) and Zn(II) complexes of both the ligands respectively is due to M–Cl bands. The broad band due to co-ordinated water molecule appeared at 3411 and 3388 cm^{-1} and 3411 and 3435 cm^{-1} in the Cu(II) and Zn(II) complexes of ligands **1** and **2** respectively.

3.2. *^{1}H NMR spectral data*

The ^{1}H NMR data of the synthesized ligands and their Zn(II) complexes are presented in Table 3. The ^{1}H NMR spectra of the ligands **1** and **2** displayed three singlets each at 12.62, 12.18 and 12.04 ppm and 12.68, 11.93 and 11.80 ppm, respectively, due to the proton of phenolic OH, amide NH and indole NH of ligands **1** and **2**, respectively. The signals due to proton of azomethine function have appeared at 8.85 and 8.86 ppm in both the ligands **1** and **2**. The aromatic protons of each of the ligands **1** and **2** have resonated as multiplets in the region 7.31–7.72 ppm (m, 10H, ArH) and 6.96–7.40 ppm (m, 10H, ArH). Three protons of the methyl group attached to 4-position of coumarin moiety have resonated as distinct singlets at 2.40 and 2.40 ppm in both ligands, respectively. Three protons of the methyl group attached to 5-position of indole moiety of ligand **2** have appeared as distinct singlet at 2.39 ppm.

In the case of Zn(II) complexes, the absence of signal due to proton of two phenolic OH groups confirms the involvement of bonding of the phenolic oxygen atom to metal ion *via* deprotonation. The signals appeared at 12.27 and 12.11 ppm, 12.05 and 11.89 ppm, 8.87 and 8.95 ppm, 7.33–7.74 and 6.98–7.61 ppm and 2.40 and 2.53 ppm are due to amide NH proton, indole NH proton, azomethine proton, aromatic protons and three protons of the methyl group attached to 4-position of coumarin moiety in each of Zn(II) complexes of ligands **1** and **2**, respectively. Singlet appeared at 2.40 ppm in case of Zn(II) complex of ligand **2** is due to three protons of the

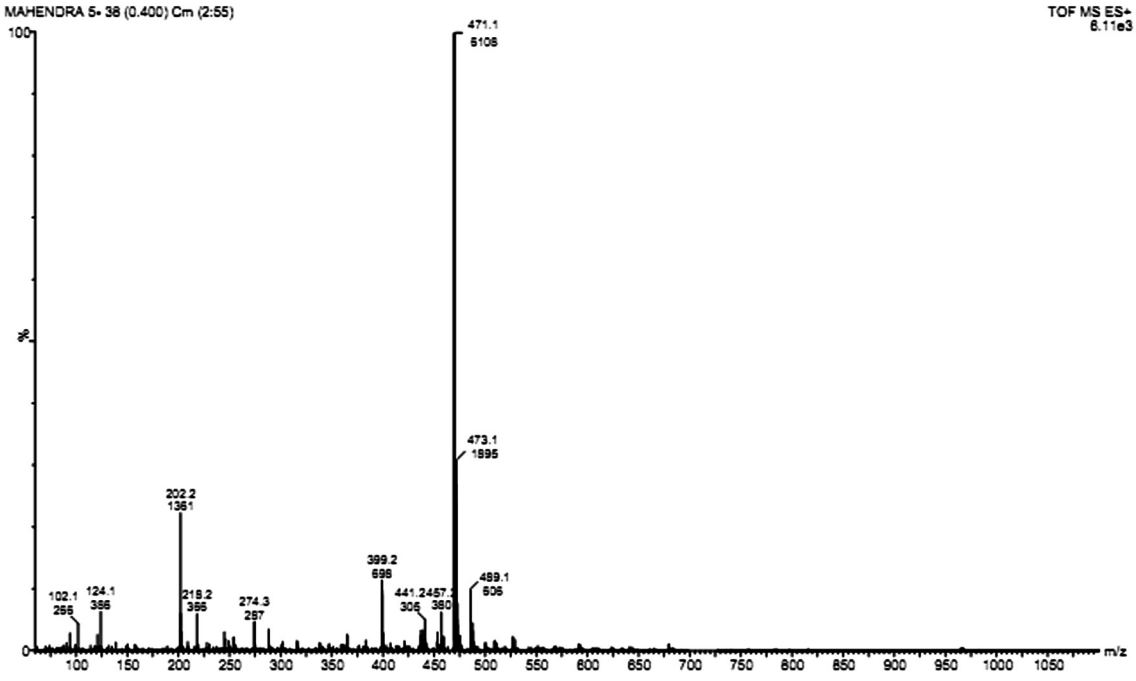

Figure 1 ESI mass spectrum of ligand **1**.

methyl group attached to 5-position of the indole moiety. When compared to the ^{1}H NMR spectra of ligands **1** and **2** and their Zn(II) complexes, all the signals due to protons have been shifted toward down field strength confirming the complexation of Zn(II) ions with the ligands. Thus the ^{1}H NMR data support the structures of ligands and their complexes.

3.3. ESI-mass spectral data

Mass spectral data confirms the structure of the ligands and the complexes as indicated by the peaks corresponding to their molecular mass. Ligands **1** and **2** and Cu(II), Co(II) and Zn(II) complexes of ligand **1** have been studied for their mass spectral studies. The ESI-mass spectra of the compounds exhibited molecular ion peaks equivalent of their molecular weight along with other fragmentation peaks. The representative mass spectrum of ligand **1** (Fig. 1) shows molecular ion peak due to $_M^{\ddagger}$ at *m*/*z* 471, 473 (100%, 30%) which is equivalent to its molecular weight and is also a base peak. This on loss of CO molecule and two hydrogen radicals gave a peak recorded at *m*/*z* 441, 443 (6%, 1.5%). Further, this on simultaneous loss of $C_{14}H_7NCl$ radical and methyl radical gave a fragment ion peak at 202 (25%), which on expulsion of C_2HO radical, HCO radical, N_2 molecule and H_2 molecule gave a peak recorded at *m*/*z* 102 (6%). The molecular ion peak due to $_M^{\ddagger}$ at *m*/*z* 471, 473 (100%, 30%) has also underwent fragmentation by another route by simultaneous loss of C_2O molecule, methyl radical and hydroxyl radical giving a fragment ion peak recorded at *m*/*z* 399, 401 (13%, 4.5%). This fragmentation pattern is in consistency with its structure (supplementary data).

The mass spectrum of ligand **2** shows molecular ion peak due to $_M^{\ddagger}$ at *m*/*z* 451 (100%) which is equivalent to its molecular weight and is also a base peak. The molecular ion peak on simultaneous loss of HCO radical, hydroxyl radical, hydrogen radical and two hydrogen molecules gave a fragment ion peak at *m*/*z* 400 (7%). This fragment ion, underwent further fragmentation by two routes; one by the loss of hydrogen radical giving a fragment ion peak recorded at *m*/*z* 399 (14%) and another by loss of C_9H_2O molecule gave a fragment ion peak recorded at *m*/*z* 274 (12%). Further, the fragment ion at *m*/*z* 274 (12%) has underwent fragmentation by two routes, one by loss of CO molecule giving a fragment ion peak recorded at *m*/*z* 246 (9.5%) another by simultaneous loss of CHN_2 radical and methyl radical giving a fragment ion peak recorded at *m*/*z* 218 (13%). This fragmentation pattern (supplementary data) is in consistency with its structure of ligand **2**.

Similarly the mass spectra of Cu(II) (**1a**) (Fig. 2) and Co(II) (**1b**) complexes of ligand **1** exhibited molecular ion peak $_M^{\ddagger}$ at *m*/*z* 605, 607 (10%, 2.7%) and 998, 1000 (12%, 4.5%), respectively which corresponds to their molecular weight. The mass spectrum of Zn(II) (**1d**) complex of ligand **1** gave a molecular ion peak due to $_M^{\ddagger}+1$ at *m*/*z* 607, 609 (13%, 3.2%), which on loss of one hydrogen gave a peak at *m*/*z* 606, 608 (8%, 1%) which is equivalent to its molecular weight. The fragmentation patterns of Cu(II), Co(II) and Zn(II) complexes of ligand **1** are depicted in supplementary data.

3.4. Electronic spectral studies

The formation of metal complexes was also confirmed by electronic spectra. Electronic spectral data of the Cu(II), Co(II) and Ni(II) complexes of the ligands **1** and **2** recorded in freshly prepared DMF solution (10^{-3} M) at room temperature are given in Table 4. The Cu(II) complexes of ligands **1** and **2** displayed single broad band each with low intensity in the region 13,590–17,876 cm^{-1} (**1a**) and 13,782–17,563 cm^{-1} (**2a**). The broad band is assigned due to three transitions $^2B_{1g} \rightarrow {}^2Eg$, $^2B_{1g} \rightarrow {}^2B_{2g}$ and $^2B_{1g} \rightarrow {}^2A_{tg}$, which are of similar

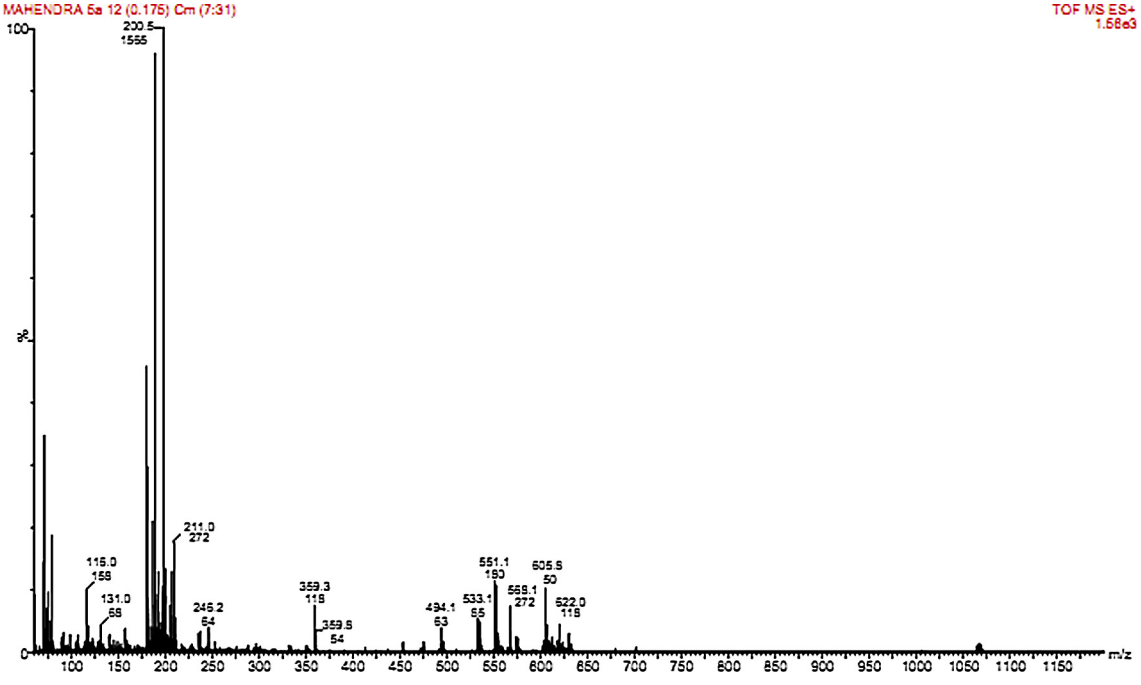

Figure 2 ESI mass spectrum of Cu(II) complex **1a**.

Table 4 Electronic spectral data and ligand field parameters of the Cu(II), Co(II) and Ni(II) complexes in DMF (10^{-3}M) solution.

Complexes	Transitions in cm^{-1}			Dq (cm^{-1})	B' (cm^{-1})	β	$\beta\%$	v_2/v_1	LFSE (k cal.)
	v_1*	v_2	v_3						
(**1a**) $[Cu(L_1)(Cl)(H_2O)_2]$	13,590–17,876			–	–	–	–	–	26.95
(**1b**) $[Co(L_1)_2]$	7912	16,982	21,237	907	967	0.929	7.01	2.14	15.54
(**1c**) $[Ni(L_1)_2]$	8210	13,598	23,874	821	855	0.822	17.78	1.65	28.14
(**2a**) $[Cu(L_2)(Cl)(H_2O)_2]$	13,782–17,563			–	–	–	–	–	26.828
(**2b**) $[Co(L_1)_2]$	7504	16,114	20,385	861	934	0.898	10.19	2.14	14.76
(**2c**) $[Ni(L_1)_2]$	8410	13,894	24,194	841	856	0.808	17.69	1.65	28.83

* Calculated values.

in energy and give rise to only single broad absorption band and the broadness of the band is due to dynamic Jahn–Teller distortion. Based on these data the Cu(II) complexes have distorted octahedral geometry [48].

The electronic spectra of Co(II) complexes of both the ligands show two absorption bands each observed at 16,982 and 21,237 cm^{-1} (**1b**) and 16,114 and 20,385 cm^{-1} (**2b**) due to two transitions $^4T_{1g}$ (F) $\rightarrow$ $^4A_{2g}$ (F) (v_2) and $^4T_{1g}$ (F) $\rightarrow$ $^4T_{2g}$ (P) (v_3) respectively. These data are in good agreement with the reported values [49]. The lowest band, v_1 was not observed due to the limited range of the instrument, it is calculated using the band fitting procedure suggested by Underhill and Billing [50]. These transitions suggest octahedral geometry for both the Co(II) complexes.

The Ni(II) complexes under present investigation exhibited two bands each in the region 13,598 and 23,874 cm^{-1} (**1c**) and 13,894 and 24,194 cm^{-1} (**2c**). These bands are assigned to $^3A_{2g}$ (F) $\rightarrow$ $^3T_{1g}$ (F) (v_2) and $^3A_{2g}$ (F) $\rightarrow$ $^3T_{1g}$ (P) (v_3) transitions respectively, in an octahedral environment. The band v_1 was calculated by using a band fitting procedure [50].

The ligand field parameters, such as the Racah inter electronic repulsion parameter (B'), ligand field splitting energy (10 Dq), nephelauxetic parameter (β) and ligand field stabilization energy (LFSE) further support the octahedral geometry of the complexes [51]. The calculated B' values for the Co(II) and Ni(II) complexes of both the ligands were lower than the free ion values, which is due to the orbital overlap and delocalization of d-orbitals. The β values are important in determining the covalency for the metal–ligand bond and they were found to be less than unity, suggesting a considerable amount of covalency for the metal–ligand bonds. The β value for the Ni(II) complexes was less than that of the Co(II) complexes, indicating the greater covalency of the M–L bond [52].

3.5. Magnetic susceptibility studies

The room temperature magnetic measurements were obtained for paramagnetic Co(II), Ni(II) and Cu(II) complexes of ligands **1** and **2** and are listed in Table 1. The observed magnetic moments for Cu(II) complexes are 1.79 BM (**1a**) and 1.80 BM (**2a**) which attributes to one unpaired electron with slight orbital contribution to the spin only value of 1.73 BM and the absence of spin–spin interactions in the complex accounting for the possibility of a distorted octahedral geometry [53]. In octahedral Co(II) complex the ground state is $^4T_{1g}$. and the orbital contribution to the singlet state lowers the magnetic moment values for the various Co(II) complexes which are in the range 4.12–4.70 and 4.70–5.20 BM for tetrahedral and octahedral complexes respectively [54]. In the present study the observed magnetic moment values for Co(II) complexes are 5.01 BM (**1b**) and 5.12 BM (**2b**) which indicate octahedral geometry for both the Co(II) complexes. For Ni(II) complexes the observed magnetic moment values are 2.90 BM (**1c**) and 2.97 BM (**2c**) which are well within the expected range for Ni(II) complex with octahedral geometry i.e. 2.83–3.50 BM [55].

3.6. ESR spectral studies of the Cu(II) complex

The ESR spectra of the Cu(II) complexes in a polycrystalline state were recorded at room temperature to elucidate the geometry and degree of covalency of the metal–ligand bond or environment around the metal ion. The X-band ESR spectra of Cu(II) complexes $[Cu(L_1)(Cl)(H_2O)_2]$ (**1a**) and $[Cu(L_2)(Cl)(H_2O)_2]$ (**2a**) have been recorded at a frequency of 9.1 GHz with a field set of 3000 G. The spin Hamiltonian parameters for the Cu(II) complex is used to derive the ground state. In octahedral geometry with the g-tensor parameter $g_\perp > g_{||} > 2.0023$, the unpaired electron lies in the d_z^2 orbital and $g_{||} > g_\perp > 2.0023$, the unpaired electron lies in the d_{x2-y2} orbital in ground state [56]. In the present study the observed measurements for Cu(II) complexes $[Cu(L_1)(Cl)(H_2O)_2]$ (**1a**), $g_{||}$ (2.154) > $g_\perp$ (2.034) > 2.0023 and $[Cu(L_2)(Cl)(H_2O)_2]$ (**2a**), $g_{||}$ (2.146) > $g_\perp$ (2.031) > 2.0023 indicate that the complex is axially symmetric and copper site has a d_{x2-y2} ground state characteristic of octahedral geometry [57]. The $g_{||}$ value is an important function for indicating the metal–ligand bond character, for covalent character $g_{||} < 2.3$ and for ionic $g_{||} > 2.3$, respectively [58]. In the present Cu(II) complexes the $g_{||}$ values were less than 2.3, indicating an appreciable covalent character for the metal–ligand bond. The geometric parameter (G), which is the measure of extent of exchange interaction is calculated by using g-tensor values by the expression $G = g_{||}-2/g_\perp-2$. According to Hathaway [59], if the G value is less than 4, the exchange interaction between the copper centers is noticed whereas if its value is greater than 4 the exchange interaction is negligible. The calculated G-values for the present Cu(II) complexes are 4.43 (**1a**) and 4.65 (**2a**) respectively indicate that the exchange coupling effects are not operative in the present complexes.

3.7. Thermal studies

The thermal behavior of Cu(II), Co(II), Ni(II) and Zn(II) complexes of ligand **1** was investigated as a function of

Table 5 Thermal data of the complexes of ligand **1**.

Complex No.	Decomposition temp (°C)	% Weight loss		% Metal oxide		Inference
		Obsd.	Cald.	Obsd.	Cald.	
1a	271	6.32	5.95	–	–	Loss due to two coordinated water molecules
	376	17.88	16.53	–	–	Loss due to CO_2 molecule, the CH_3 group and a Cl atom
	388	35.48	33.92	–	–	Loss due to C_9H_4N moiety and a Cl atom
	Up to 715	–	–	13.28	13.15	Loss due to remaining organic moiety
1b	312	12.52	11.82	–	–	Loss due to two CO_2 molecules and two CH_3 groups
	383	9.09	7.94	–	–	Loss due to two Cl atoms
	426	37.50	37.11	–	–	Loss due to two C_9H_4 moieties and a phenyl group
	Up to 715	–	–	7.36	7.50	Loss due to remaining organic moiety
1c	366	17.53	18.82	–	–	Loss due to two CO_2 molecules, two CH_3 groups and two Cl atoms
	398	42.53	44.25	–	–	Loss due to two $C_9H_5N_2$ moieties and a phenyl group
	450	22.83	24.13	–	–	Loss due to a phenyl group and O_2 molecule
	Up to 715	–	–	7.58	7.47	Loss due to remaining organic moiety
1d	204	4.92	5.93	–	–	Loss due to two coordinated water molecules
	352	13.07	13.84	–	–	Loss due to CO_2 molecule and a Cl atom
	441	48.34	46.80	–	–	Loss due to $C_{14}H_9NCl$ and two H_2 molecules
	Up to 715	–	–	13.48	13.42	Loss due to remaining organic moiety

temperature. The suggested stepwise thermal degradation of the complexes with respect to temperature and the formation of respective metal oxides are depicted in Table 5. Thermogravimetic–differential thermal analysis curve of Cu(II) complex (**1a**) (Fig. 3) shows that the complex is stable up to 270 °C and no weight loss occurs before this temperature and underwent decomposition in three successive steps. The first stage of decomposition represents weight loss of coordinated water molecules at 271 °C with practical weight loss of 6.32% (Cald. 5.95%). The resultant complex underwent second stage of degradation and gave break at 376 °C with a practical weight loss of 17.88% (Cald. 16.53%), which corresponds to the decomposition of CO_2 molecule, the methyl group and a chlorine atom. Further the complex underwent third stage of

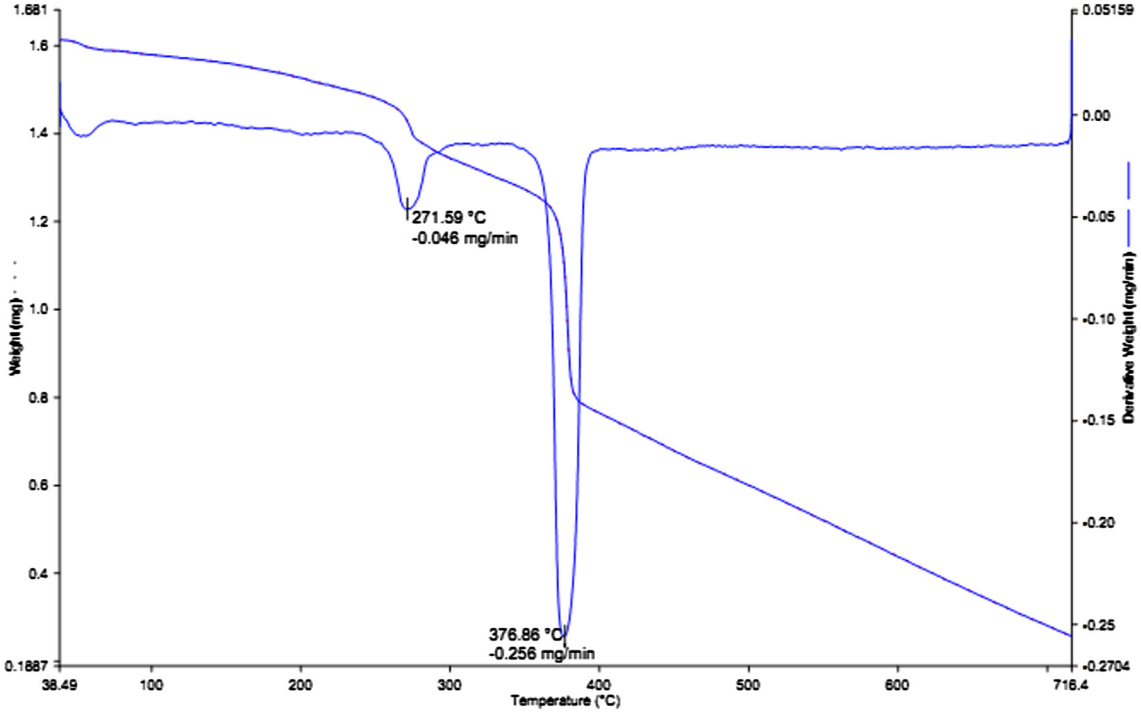

Figure 3 TG–DTA curve of Cu(II) complex **1a**.

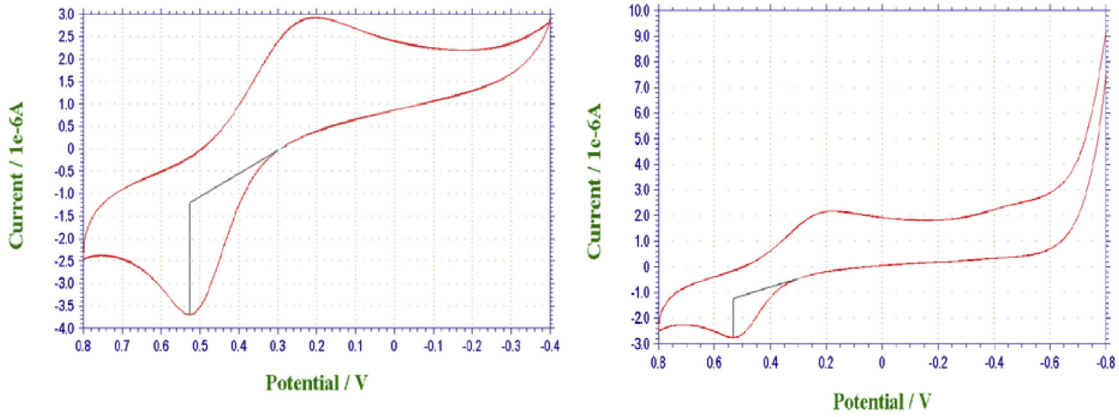

1a $[Cu(L_1)(Cl)(H_2O)_2]$ **2a** $[Cu(L_2)(Cl)(H_2O)_2]$

Figure 4 Cyclic voltammogram of Cu(II) complexes at scan rate of 0.1 Vs^{-1}.

decomposition and gave a break at 388 °C with a weight loss of 35.48% (Cald. 33.92%) due to loss of C_9H_4N moiety and a chlorine atom. Thereafter, the compound showed a gradual decomposition in a gradual manner rather than with the sharp decomposition up to 715 °C and onwards due to the loss of the remaining organic moiety. The weight of the residue corresponds to cupric oxide.

The thermogram of Co(II) complex (**1b**) shows the first stage of decomposition at 312 °C with practical weight loss of 12.52% (Cald. 11.82%), which corresponds to weight loss of two CO_2 molecules and two CH_3 groups. Further the complex underwent decomposition and gave a break at 383 °C with a practical weight loss of 9.09% (Cald. 7.94%), corresponds to weight loss of two Cl atoms. The resultant complex underwent third stage of decomposition at 426 °C with the weight loss of 37.50% (Cald. 37.11%) due to loss of two C_9H_4 moieties and a phenyl group. Thereafter the complex showed gradual decomposition up to 750 °C with a weight loss of remaining organic moiety, the weight of the residue corresponds to cobalt oxide.

In the thermogram of the Ni(II) complex (**1c**), the first stage of decomposition represents the weight loss of two CO_2 molecules, two CH_3 groups and two Cl atoms at 366 °C with a practical weight loss of 17.53% (Cald. 18.82%). The resultant complex underwent further degradation and gave break at 398 °C with a practical weight loss of 42.53% (Cald. 44.25%), which corresponds to the decomposition of two $C_9H_5N_2$ moieties and a phenyl group. Further the resulting complex underwent decomposition and gave a break at 450 °C with a practical weight loss of 22.83% (Cald. 24.13), which corresponds to the weight loss of a phenyl group and an O_2 molecule. Thereafter, the compound showed a gradual decomposition up to 715 °C with a weight loss of remaining organic moiety. The weight of the residue corresponds to nickel oxide.

In case of Zn(II) complex (**1d**) the first stage of decomposition occurs at 204 °C with practical weight loss of 4.92% (Cald. 5.93%), which represents the loss due to two coordinated water molecules. Further the complex underwent second stage of decomposition and gave a break at 352 °C with practical weight loss of 13.07% (Cald. 13.84%), due to loss of CO_2 molecule and a chlorine atom. The third stage of decomposition occurs at 441 °C with practical weight loss of 48.34% (Cald. 46.80%), due to loss of $C_{14}H_9NCl$ moiety and two hydrogen molecules. Thereafter, the compound showed a gradual decomposition up to 715 °C with the weight loss of the remaining organic moiety. The weight of the residue corresponds to zinc oxide. The percentage metal content in all the complexes as done by elemental analysis agrees well with the thermal studies.

3.8. Electrochemistry

Electrochemical methods offer the potential to determine the number of electrons involved in the redox process. The electrode potential at which the complex undergoes oxidation or reduction can be rapidly located by cyclic voltammetry. The redox behavior of all the complexes was investigated in DMF (10^{-3} M) solution containing 0.05 M tetrabutylammonium perchlorate as a supporting electrolyte in an oxygen free condition using a glassy carbon working electrode by cyclic voltammetry, which is the most versatile electro analytical technique for the study of electroactive species. Only the Cu(II) complexes of both the ligands exhibited redox properties. The voltammogram of two Cu(II) complexes are shown in Fig. 4. The cyclic voltammogram of Cu(II) complex (**1a**) in DMF at a scan rate of 0.1 Vs^{-1} shows well defined redox process corresponding to the formation of Cu(II)/Cu(I) couple at (reduction peak) E_{pc} = 0.220 V and (oxidation peak) E_{pa} = 0.527 V versus Ag/AgCl. The peak separation of this couple is found to be quasi-reversible with ΔE_p = 0.307 V and the ratio of anodic to cathodic peak height was less than one. The difference between forward and backward peak potential can provide a rough evaluation of the degree of the reversibility of one electron transfer reaction. Thus, the analysis of cyclic voltammetric response to 0.1, 0.15 and 0.2 Vs^{-1} scan rates gives the evidence for quasi-reversible one electron redox process. The ratio of anodic to cathodic peak height was less than one and peak current increases with the increase of square root of the scan rates, establishing diffusion controlled electrode process [60]. From the peak separation value ΔE_p and peak potential which increase with higher scan rates, we can suggest that the electrode process are consistent with the quasi-reversibility of Cu(II)/Cu(I) couple [61].

The Cu(II) complex (**2a**) exhibits the reduction peak at $E_{pc} = 0.200$ V with the corresponding oxidation peak $E_{pa} = 0.533$ V, which corresponds to the formation of Cu(II)/Cu(I) couple. The peak separation of this couple is $\Delta E_p = 0.333$ V which increases with increasing scan rates. These characteristics are in consistency with the quasi-reversibility of Cu(II)/Cu(I) couple.

3.9. Powder X-ray diffraction studies (Powder-XRD)

Crystals that are suitable for single-crystal studies were not obtained since all the metal complexes are not soluble in common organic solvents but soluble in some polar solvents like DMF and DMSO. Hence powder-XRD pattern of metal complexes of the ligand **1** has been studied in order to test the degree of crystallinity of the complexes. Powder X-ray diffraction pattern for Cu(II) complex (**1a**) showed 14-reflections in the range of 6–56° (2θ), which arose from diffraction of X-ray by the planes of complex. The interplanar spacing (d) has been calculated by using Bragg's equation, $n\lambda = 2d \sin\theta$. The calculated interplanar d-spacing together with relative intensities with respect to most intense peak have been recorded and depicted in Table 6. The unit cell calculations have been calculated for cubic symmetry from the entire important peaks and $h^2 + k^2 + l^2$ values were determined. The observed interplanar d-spacing values have been compared with the calculated ones and it was found to be in good agreement. The $h^2 + k^2 + l^2$ values are 1, 12, 14, 17, 18, 20, 27, 28, 35, 45, 51, 56, 76, and 82. It was observed that the presence of forbidden number 28 indicates that the Cu(II) complex may belong to hexagonal or tetragonal systems.

Similar calculations were performed for Co(II), Ni(II) and Zn(II) complexes of ligand **1**. The Co(II) (**1b**) and Ni(II) (**1c**) complexes showed 9- reflections each, whereas Zn(II) complex showed 16-reflections each in the range 3–75° (2θ), respectively, which arose from the diffraction of X-ray by the planes of these complexes. All the important peaks of Co(II), Ni(II) and Zn(II) complexes have been indexed and observed values of interplanar distances (d) have been compared with the calculated ones and it was found to be in good agreement. The

Table 6 Powder X–ray diffraction data of Cu(II) complex of ligand **1**.

Peak	2θ	θ	Sinθ	Sin$^2\theta$	1000 Sin$^2\theta$	1000 Sin$^2\theta$/CF ($h^2 + k^2 + l^2$)	*hkl*	*d*		*a* in Å
								Obsd.	Cald.	
1	6.015	3.0075	0.0524	0.0027	2.70	1.00(1)	100	14.681	14.694	14.818
2	21.142	10.571	0.1834	0.0336	33.60	12.44(12)	222	4.1989	4.1984	14.815
3	22.243	11.121	0.1928	0.0371	37.17	13.76(14)	321	3.9935	3.9937	14.819
4	24.643	12.321	0.2133	0.0454	45.40	16.81(17)	322	3.6096	3.6099	14.816
5	25.820	12.910	0.2234	0.0499	49.90	18.48(18)	330	3.4477	3.4467	14.818
6	26.904	13.452	0.2326	0.0541	54.10	20.03(20)	420	3.3113	3.3104	14.816
7	31.212	15.606	0.2690	0.0723	72.30	26.77(27)	333/511	2.8633	2.8624	14.816
8	32.118	16.059	0.2766	0.0765	76.50	28.33(28)	–	2.7846	2.7838	14.817
9	35.597	17.798	0.3056	0.0933	93.30	34.55(35)	531	2.5200	2.5196	14.817
10	40.789	20.394	0.3484	0.1213	121.30	44.92(45)	630	2.2104	2.2101	14.817
11	43.527	21.763	0.3707	0.1374	137.40	50.88(51)	711	2.0775	2.0771	14.817
12	45.884	22.942	0.3897	0.1518	151.80	56.22(56)	642	1.9761	1.9758	14.807
13	53.844	26.922	0.4527	0.2049	204.90	75.88(76)	662	1.7012	1.7009	14.817
14	56.127	28.063	0.4704	0.2212	221.20	81.92(82)	910	1.6373	1.6369	14.818

Table 7 Minimum inhibitory concentration (MIC μg mL^{-1}) of ligands (**1** and **2**) and their metal complexes.

Compound	Bacteria				Fungi		
	B. subtilis	*S. typhi*	*E. coli*	*S. aureus*	*A. niger*	*C. albicans*	*C. oxysporum*
1	50	100	50	50	50	50	50
2	75	100	75	100	75	100	75
1a	12.50	25	12.50	12.50	12.50	25	25
1b	25	75	25	25	25	12.50	12.50
1c	25	75	25	25	25	25	25
1d	25	75	25	25	25	25	25
2a	25	75	25	50	25	50	50
2b	25	75	50	50	50	50	25
2c	25	75	50	50	50	75	50
2d	50	75	50	75	50	75	50
$Cucl_2.2H_2O$	>100	>100	>100	>100	>100	>100	>100
$Cocl_2.6H_2O$	>100	>100	>100	>100	>100	>100	>100
$Nicl_2.6HO$	>100	>100	>100	>100	>100	>100	>100
$Zncl_2$	>100	>100	>100	>100	>100	>100	>100
Gentamicin	12.50	12.50	12.50	12.50	–	–	–
Fluconazole	–	–	–	–	12.50	12.50	12.50

unit cell calculations were performed for cubic system and the $h^2 + k^2 + l^2$ values were determined for the above complexes. The Co(II) (**1b**) complex showed the absence of forbidden numbers (7, 15, 23, 71 etc.) which indicates that complexes have cubic symmetry. The calculated lattice parameters for Co(II) complex were $a = b = c = 3.36$ Å, whereas for Ni(II) (**1c**) and Zn(II) (**1d**) complexes, it was observed that the presence of forbidden numbers 23 and 71 for Ni(II) complexes and 28, 123 and 210 for Zn(II) complexes indicates that the both complexes may belong to hexagonal or tetragonal systems.

3.10. Pharmacological results

3.10.1. In vitro antimicrobial activity

The synthesized ligands (**1** and **2**) and their metal complexes have been screened for their antimicrobial activity. The antibacterial activity of the synthesized compounds was tested for their effect on *E. coli*, *S. typhi*, *B. subtilis* and *S. aureus* bacterial strains and antifungal activity was tested on *C. albicans*, *C. oxysporum* and *A. niger* fungal strains. Minimum inhibitory concentration (MIC) values of the compounds against the respective strains are summarized in Table 7. The antimicrobial screening results of all the synthesized compounds exhibited antimicrobial properties and it is important to note that the metal complexes exhibited more inhibitory effect compared to their respective parent ligands and their metal chlorides. Due to the presence of the electron withdrawing group, the chloro substituted compounds showed better zone of inhibition compared to methyl substituted compounds. The enhanced antimicrobial activity of the complexes over the ligands and their respective metal chlorides can be explained on the basis of the chelation theory [62,63]. It is known that chelation enhances the ligand to act as more powerful and potent bactericidal agents by inhibiting the bacterial growth, thus zone of inhibition of metal complexes was found to be higher compared to their free ligands. The enhancement in the activity may be rationalized on the basis that ligands mainly possess azomethine (C═N) bond. More over in metal complex, the positive charge of the metal ion is partially shared with the hetero donor atoms (nitrogen and oxygen) present in the ligand, and there may be π-electron delocalization over the whole chelating system [64,65]. Hence the increase in the lipophilic character of the metal chelates favors its permeation through the lipoid layer of the bacterial membranes and blocking of the metal binding sites in the enzymes of microorganisms. The other factors such as conductivity, solubility and bond length between the ligand and the metal ion also increase the activity.

3.10.2. Antioxidant assay (DPPH free radical scavenging activity)

The free radical scavenging activity of ligand **1** and its metal complexes was done by the DPPH method. Antioxidant activity of the test compounds was examined by measuring radical scavenging effect of DPPH radicals. The results of the free radical scavenging activity of the compounds at different concentrations are shown in Fig. 5 and IC_{50} values of the test compounds are depicted in Table 8. It was observed that the free radical scavenging activity of these compounds was concentration dependent. Among the examined compounds ligand **1** and its Cu(II), Co(II) and Ni(II) complexes have exhibited good scavenging activity, whereas Zn(II) complex has showed moderate activity. The antioxidant activity of the ligand **1** was comparatively high when compared to all the metal complexes and is due the presence of the phenolic OH group and the marked antioxidant activity of metal complexes is due to the coordination of metal with azomethine nitrogen, carbonyl oxygen of amide function attached to the 2-position of indole and phenolic oxygen of coumarin moiety *via* deprotonation. In

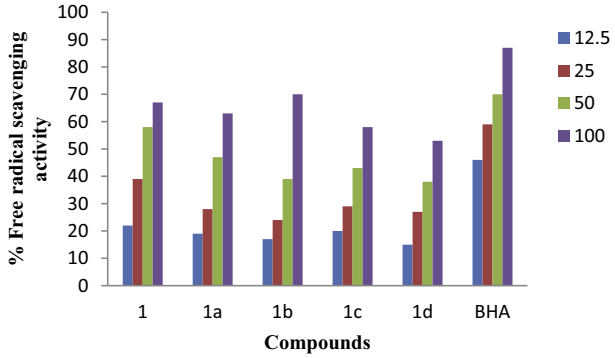

Figure 5 Antioxidant activity results of ligand **1** and its complexes.

Table 8 IC_{50} values of DPPH radical scavenging activity of ligand **1** and its complexes.

Compounds	IC_{50} values (μg mL^{-1})
1	54.10
1a	68.78
1b	67.68
1c	76.49
1d	88.48

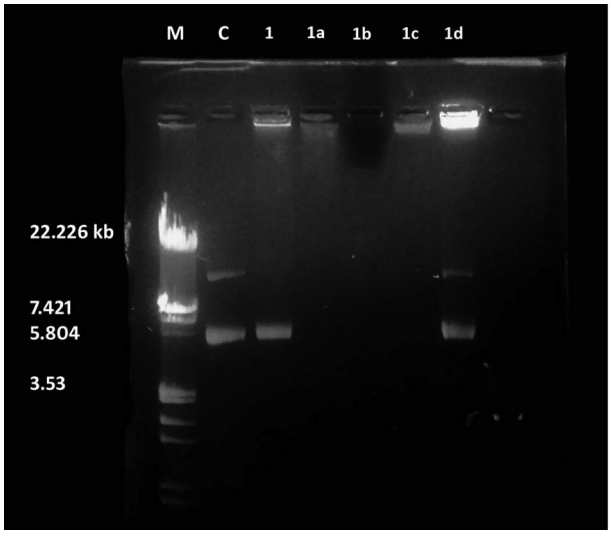

Figure 6 DNA cleavage of supercoiled plasmid DNA pBR322. **M**, standard molecular weight marker; **C**, control. Lane **1**, **1a**, **1b**, **1c**, and **1d** were treated plasmid DNA pBR322 with respective compounds.

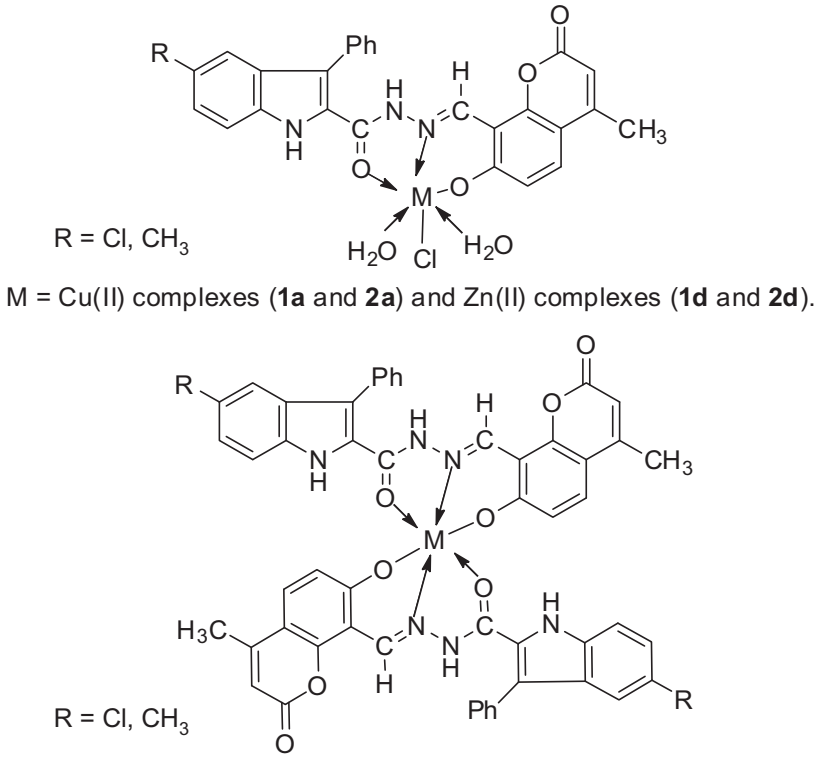

Figure 7 Proposed structures of the complexes.

case of the ligand **1** hydrogen of the OH group donates to the DPPH and converts itself into the stable free radical and in metal complexes the hydrogen of azomethine is more acidic than the hydrogen of the indole NH. Hence, hydrogen of azomethine could be easily donated to the DPPH free radical and converts itself into the stable free radical. Moreover, the acidic nature of hydrogen atom attached to azomethine nitrogen increases on complexation with metal ions. Hence hydrogen atom becomes more liable.

3.10.3. DNA cleavage activity

The ligand **1** and its Cu(II), Co(II), Ni(II) and Zn(II) complexes were studied for their DNA cleavage activity by the agarose gel electrophoresis method against supercoiled plasmid DNA pBR 322 (Bangal re Genei, Bengaluru, Cat. No. 105850) as a target molecule and the gel picture showing cleavage is depicted in Fig. 6.

DNA-cleavage studies are used to construct new and rational design of more efficient drugs that are targeted to DNA [66]. The metal complexes were able to convert supercoiled DNA into open circular DNA. Treatment of DNA on the complexes revealed that, all the complexes have acted on DNA as there was molecular weight difference between the treated DNA samples and the control. The difference was observed in bands of lanes compared to the control DNA pBR 322. The results indicate the important role of nitrogen and oxygen atoms to the metal ions in these isolated DNA cleavage reactions. On the basis of the cleavage of DNA observed in case of ligand **1** and its Cu(II), Co(II), Ni(II) and Zn(II) complexes, it can be concluded that all the compounds under the present study inhibited the growth of pathogenic organism by DNA cleavage as has been observed on the DNA cleavage of supercoiled plasmid DNA pBR 322.

4. Conclusions

Based on the spectroscopic studies, the coordinating ability of the ligands has been proved in complexation reaction with Cu(II), Co(II), Ni(II) and Zn(II) ions. The newly synthesized ligands act as an ONO donor tridentate chelate around the metallic ion. Metal ion is coordinated through oxygen atom of carbonyl function, azomethine nitrogen and phenolic oxygen atom *via* deprotonation. Cu(II), Co(II), Ni(II) and Zn(II) complexes of both the ligands possess octahedral geometries. Cu(II) complexes of ligands **1** and **2** exhibit one electron transfer quasi-reversible redox activity in the applied potential range. The antimicrobial activity results showed that all the complexes have exhibited higher activity when compared to their respective ligands. Ligand **1** showed efficient antioxidant activity compared to their complexes. The electrophoretic studies indicated that all the metal complexes have good efficiency toward DNA cleavage. From the present study, it can be concluded that other ligands containing indole and coumarin derivatives and their metal complexes can be synthesized and characterized which will give valuable information in the field of coordination and inorganic chemistry about the bonding modes and elucidating various structures. Based on the analytical data and spectral studies, proposed structures of all the complexes are depicted in Fig. 7.

Acknowledgments

Authors are thankful to the Professor and Chairman, Department of Chemistry, Gulbarga University, Gulbarga for providing the laboratory facilities. We are grateful to SAIF Punjab University, Chandigarh, STIC Cochin University, for providing spectral and analysis data and BioGenics Research and Training Centre in Biotechnology, Hubli for biological activities.

Appendix A. Supplementary data

Supplementary data associated with this article can be found, in the online version, at http://dx.doi.org/10.1016/j.jscs.2014.01.001.

References

[1] M.J. Clarke, Ruthenium metallopharmaceuticals, Coord. Chem. Rev. 236 (2003) 209–233.
[2] C.G. Hartinger, P.J. Dyson, Bioorganometallic chemistry—from teaching paradigms to medicinal applications, Chem. Soc. Rev. 38 (2009) 391–401.
[3] M. Navarro, Gold complexes as potential anti-parasitic agents, Coord. Chem. Rev. 253 (2009) 1619–1626.
[4] K. Selmeczi, M. Giorgi, G. Speier, E. Farkas, M. Reglier, Mono-versus binuclear Copper(II) complexes in phosphodiester hydrolysis, Eur. J. Inorg. Chem. 2006 (2006) 1022–1031.
[5] N.H. Williams, B. Takasaki, M. Wall, J. Chin, Structure and nuclease activity of simple dinuclear metal complexes: quantitative dissection of the role of metal ions, Acc. Chem. Res. 32 (1999) 485–493.
[6] G. Roelfes, M.E. Branun, L. Wang, L. Que, B.L. Feringa, Efficient DNA cleavage with an iron complex without added reductant, J. Am. Chem. Soc. 122 (2000) 11517–11518.
[7] M. Sam, J.H. Hwang, G. Chanfreau, M.M. Abu-Omar, Hydroxyl radical is the active species in photochemical DNA strand scission by Bis(peroxo)vanadium(V) phenanthroline, Inorg. Chem. 43 (2004) 8447–8455.
[8] L. Liu, J.J. Huang, J. Zhang, G. Liu, X. Wang, H. Lin, N. Chen, Y. Qu, Polycarboxylate-assisted assembly of cobalt(II) metal–organic coordination polymers from a ''V''-shaped tri-pyridyl-bis-amide ligand, Trans. Met. Chem. 27 (2002) 689–697.
[9] I. Avan, G. Alaattin, G. Kiymet, Synthesis and antimicrobial investigation of some 5*H*-pyridazino[4,5-b]indoles, Turk. J. Chem. 37 (2013) 271–291.
[10] S.S. El-Nakkady, S.E.-S. Abbas, H.M. Roaiah, I.H. Ali, Synthesis, antitumor and anti-inflammatory activities of 2-thienyl-3-substitued indole derivatives, Global J Pharm. 6 (3) (2012) 166–177.
[11] P. Rani, V.K. Srivastava, K. Ashok, Synthesis and anti-inflammatory activity of heterocyclic indole derivatives, Eur. J. Med. Chem. 39 (2004) 449–452.
[12] A.H. Mandour, E.R. El-sawy, K.H. Shaker, M.A. Mustafa, Synthesis, anti-inflammatory, analgesic and anticonvulsant activities of 1,8-dihydro-1-aryl-8-alkyl pyrazolo(3,4-b)indoles, Acta Pharm. 60 (2010) 73–88.
[13] H. Chai, Y. Zhao, C.P. Gong, Synthesis and *in vitro* anti-hepatitis B virus activities of some ethyl 6-bromo-5-hydroxy-1*H*-indole-3-carboxylates, Bioorg. Med. Chem. 14 (2006) 911–917.
[14] N. Karali, A. Gursoy, F. Kandemirli, N. Shvets, F.B. Kaynak, S. Ozbey, V. Kovalishyn, A. Dimoglo, Synthesis and structure-antituberculosis activity relationship of 1*H*-indole-2,3-dione derivatives, Bioorg. Med. Chem. 15 (17) (2007) 5888–5904.
[15] A.S. Kalgutkar, B.C. Crews, S. Saleh, D. Prudhomnae, L. Marnett, Indolyl esters and amides related to indomethacin are selective COX-2 inhibitors, J. Bioorg. Med. Chem. 13 (2005) 6810–6822.
[16] S. Olgen, D. Nebioglu, Synthesis and biological evaluation of N-substituted indole esters as inhibitors of cyclo-oxygenase-2 (COX-2), IL Farmaco 57 (2002) 677–683.
[17] N. Ergenc, N.S. Gunay, R. Demirdamar, Synthesis and antidepressant evaluation of new 3-phenyl-5-sulfon-amidoindole derivatives, Eur. J. Med. Chem. 33 (1998) 143–148.
[18] A.Y. Merwade, S.B. Rajur, L.D. Basngoudar, Synthesis and antiallergic activities of 10-substituted-4-chloro-12-methyl(or phenyl)-1,2-dihydroqunoxalino[1, 2′a]indoles, Indian J. Chem. Sec. B 29 (1990) 1113–1117.
[19] S. Vikas, K. Pradeep, P. Devender, Biological importance of the indole nucleus in recent years: a comprehensive review, J. Hetero. Chem. 47 (3) (2010) 491–502.
[20] S.M.S. Chauhan, P.P. Mohapatra, T.S. Kohli, S. Satapaty, Biomimetic oxidation of indole-3-acetic acid and related substrates with hydrogen peroxide catalysed by 5,10,15,20-tetrakis 2′,6′-dichloro-3′-sulfonatophenyl)porphyrinatoiron(III) hydrate in aqueous solution and AOT reverse micelles, J. Mol. Catal. A: Chem. 113 (1–2) (1996) 239–247.
[21] B. Sandhya, D. Giles, V. Mathew, G. Basavarajaswamy, R. Abraham, Synthesis, pharmacological evaluation and docking studies of coumarin derivatives, Eur. J. Med. Chem. 46 (9) (2011) 4696–4701.
[22] A.A. Emmanuel-Giota, K.C. Fylaktakidou, D.J. Hadjipavlou-Litina, K.E. Litinas, D.N. Nicolaides, Synthesis and biological evaluation of several 3-(coumarin-4-yl)tetrahydroisoxazole and 3-(coumarin-4-yl)dihydropyrazole derivatives, J. Heterocycl. Chem. 38 (3) (2001) 717–722.
[23] P. Laurin, D. Ferroud, M. Klich, C. Dupis-Hamlin, P. Mauvais, P. Lassaigne, A. Bonnefoy, B. Musicki, Synthesis and *in vitro* evaluation of novel highly potent coumarin inhibitors of gyrase B, Bioorg. Med. Chem. Lett. 9 (14) (1999) 2079–2084.
[24] Z.M. Nofal, M. El-Zahar, S. Abd El-Karim, Novel coumarin derivatives with expected biological activity, Molecules 5 (2000) 99–113.
[25] S. Kirkiacharian, D.T. Thuy, S. Sicsic, R. Bakhchinian, R. Kurkjian, T. Tonnaire, Structure–activity relationships of some 3-substituted-4-hydroxycoumarins as HIV-1 protease inhibitors, IL Farmaco 57 (9) (2002) 703–708.
[26] D. Yu, M. Suzuki, L. Xie, S.L. Morris-Natschke, K.H. Lee, Recent progress in the development of coumarin derivatives as potent anti-HIV agents, Med. Res. Rev. 23 (3) (2003) 322–345.
[27] Lin. Mei-Hsiang, Chou. Yu-Shiang, Tsai. Yan-Jyu, Chau. Duen-Suey, Antioxidant properties of 5,7,-dihyroxy coumarin derivatives in vitro cell-free and cell containing system, J. Exp. Clin. Med. 3 (3) (2011) 126–131.
[28] P. Bermejo, E. Pinero, A.M. Villar, Iron-chelating ability and antioxidant properties of phycocyanin isolated from a protean extract of *Spirulinaplatensis*, Food Chem. 110 (2008) 436–445.
[29] C. Sanja, K. Franci, M. Milka, Synthesis and antioxidant activity of selected 4-methylcoumarins, Food Chem. 177 (1) (2009) 135–142.
[30] M.E. Buyukokuroglu, I. Gulcin, M. Oktay, O.I. Kufrevioglu, *In vitro*-antioxidant properties of dantrolene sodium, Pharmacol. Res. 44 (2001) 491–494.
[31] M.E. Bravo-Gomez, J.C. Garcia-Ramos, I. Gracia-Mora, L. Ruiz-Azuara, Antiproliferative activity and QSAR study of copper(II) mixed chelate [Cu(N–N)(acetylacetonato)]NO_3 and [Cu(N–N)(glycinato)]NO_3 complexes, (Casiopeínas), J. Inorg. Biochem. 103 (2009) 299–309.
[32] Y. Jadegoud, O.B. Ijare, N.N. Mallikarjun, S.D. Angadi, B.H.M. Mruthyunjayaswamy, Synthesis and antimicrobial

activity of Copper-, Cobalt- and Nickel(II) complexes with Schiff bases, J. Indian Chem. Soc. 79 (2002) 921–924.
[33] Y. Jadegoud, O.B. Ijare, B.S. Somashekar, G.A. Naganagowda, B.H.M. Mruthyunjayaswamy, Synthesis, characterization and antimicrobial activity of homodinuclear complexes derived from 2,6-*bis*[3′-methyl-2′-carboxamidyliminomethyl(6′,7′)benz indole]-4-methylphenol, an end-off compartmental ligand, J. Coord. Chem. 61 (4) (2008) 508–527.
[34] K. Mahendra Raj, B. Vivekanand, B.H.M. Mruthyunjayaswamy, Synthesis, characterization, antimicrobial, DNA cleavage, and antioxidant studies of some metal complexes derived from Schiff base containing indole and quinoline moieties, Bioinorg. Chem. Appl. 2013 (2013) 1–16.
[35] B.H.M. Mruthyunjayaswamy, O.B. Ijare, Y. Jadegoud, Synthesis, characterization and biological activity of symmetric dinuclear complexes derived from a novel macrocyclic compartmental ligand, J. Braz. Chem. Soc. 16 (2005) 783–789.
[36] B.H.M. Mruthyunjayaswamy, Y. Jadegoud, O.B. Ijare, S.G. Patil, S.M. Kudari, Synthesis, characterization and antimicrobial activity of macrocyclic phenoxo-bridged di- and tetra-nuclear complexes from N, N-bis[2,6-diiminomethyl-4-methyl-1-hydroxyphenyl]succinoyl/sebacoyldicarboxamides, Trans. Met. Chem. 30 (2005) 234–242.
[37] F. Rahaman, B. Hiremath, S.M. Basavarajaiah, B.H.M. Jayakumarswamy, B.H.M. Mruthyunjayaswamy, Synthetic, spectral, thermal and antimicrobial activity studies of some transition metal complexes derived from 2-hydroxy methylbenzaldehyde N-(4′-phenyl-1′,3′-thiazol-2′-yl)semicarbazone, J. Indian Chem. Soc. 85 (2008) 381–386.
[38] F. Rahaman, O.B. Ijare, Y. Jadegoud, B.H.M. Mruthyunjayaswamy, Phenoxo-bridged symmetrical homobinuclear complexes derived from an "End-Off" compartmental ligand, 2,6-bis[5′-chloro-3′-phenyl-1*H*-indole-2′-carboamidyliminomethyl]-4-methylphenol, J. Coord. Chem. 1 (2009) 1–11.
[39] A.I. Vogel, A Text Book of Quantitative Inorganic Analysis, third ed., ELBS, Longman, London, 1968.
[40] S.P. Hiremath, B.H.M. Mruthyunjayaswamy, M.G. Purohit, Synthesis of substituted 2-aminoindolees and 2-(2′-phenyl-1′,3′,4′-oxadiazolyl) aminoindoles, Indian J. Chem. Sec. B 16B (1978) 789–792.
[41] A. Kulkarni, S.A. Patil, P.S. Badami, Synthesis, characterization, DNA cleavage and in vitro antimicrobial studies of La(III), Th(IV) and VO(IV) complexes with Schiff bases of coumarin derivatives, Eur. J. Med. Chem. 44 (2009) 2904–2912.
[42] R.P. Singh, K.N.C. Murthy, G.K. Jayaprakasha, Studies on the antioxidant activity of pomegranate (*Punica granatum*) peel and seed extracts using in vitro models, J. Agric. Food Chem. 50 (2002) 81–86.
[43] J. Sambrook, E.F. Fritsch, T. Maniatis, Molecular cloning, A laboratory Manual, second ed., Cold Spring Harbor Laboratory, Cold Spring Harbor, New York, 1989.
[44] W.J. Geary, The use of conductivity measurements in organic solvents for the characterisation of coordination compounds, Coord. Chem. Rev. 7 (1971) 81–122.
[45] S. Roy, T.N. Mandal, K. Das, R.J. Butcher, A.L. Rheingold, S.K. Kar, Syntheses, characterization, and X-ray crystal structures of two cis-dioxovanadium(V) complexes of pyrazole-derived, Schiff-base ligands, J. Coord. Chem. 63 (2010) 2146–2157.
[46] Sulekha, K.G. Lokesh, EPR, mass, IR, electronic, and magnetic studies on Copper(II) complexes of semicarbazones and thiosemicarbazones, Spectrochim. Acta Part A 61A (2005) 269–272.
[47] P.P. Dholakiya, M.N. Patel, Synthesis, spectroscopic studies, and antimicrobial activity of Mn(II), Co(II), Ni(II), Cu(II), and Cd(II) complexes with bidentate Schiff bases and 2, 2′-bipyridylamine, Synth. React. Inorg. Metal-Org. Chem. 32 (4) (2002) 753–762.
[48] A. Koji, M. Kanako, M. Ohba, H. Okawa, Site specificity of metal ions in heterodinuclear complexes derived from an "End-Off" compartmental ligand, Inorg. Chem. 41 (2002) 4461–4465.
[49] R.A. Rai, Metal complexes of 5-(o)hydroxyphenyl-1,3,4-oxadiazole-2-thione, J. Inorg. Nucl. Chem. 42 (1980) 450–453.
[50] A.E. Underhill, D.E. Billing, Calculations of the Racah parameter B for Nickel (II) and Cobalt (II) compounds, Lett. Nat. 210 (1966) 834–835.
[51] D.N. Satyanarayana, Electronic Absorption Spectroscopy and Related Techniques, University Press India Limited, New Delhi, 2001.
[52] K. Shivakumar, Shashidhar, P. Vithal Reddy, M.B. Halli, Synthesis, spectral characterization and biological activity of benzofuran Schiff bases with Co(II), Ni(II), Cu(II), Zn(II), Cd(II) and Hg(II) complexes, J. Coord. Chem. 61 (14) (2008) 2274–2287.
[53] D.P. Singh, R. Kumar, V. Malik, P. Tyagi, Synthesis and characterization of complexes of Co(II), Ni(II), Cu(II), Zn(II), and Cd(II) with macrocycle 3,4,11,12-tetraoxo-1,2,5,6,9,10,13,14-octaaza-cyclohexadeca-6,8,14,16-tetraene and their biological screening, Trans. Met. Chem. 32 (2007) 1051–1055.
[54] M.U. Hassan, Z.H. Chohan, C.T. Supuran, Antibacterial Zn(II) compounds of Schiff bases derived from some benzothiazoles, Main Group Metal Chem. 25 (2002) 291–296.
[55] T.R. Rao, P. Archan, Synthesis and spectral studies on 3d metal complexes of mesogenic Schiff base ligands. Part 1. Complexes of N-(4-butylphenyl) salicylaldimine, Synth. React. Inorg. Metal-Org. Chem. 35 (4) (2005) 299–304.
[56] S. Balasubramanian, C.N. Krishnan, Synthesis and characterization of five-coordinate macrocyclic complexes of nickel(II) and copper(II), Polyhedron 5 (3) (1986) 669–675.
[57] B.T. Thaker, P.K. Tandel, A.S. Patel, C.J. Vyas, M.S. Jesani, D.M. Patel, Synthesis and mesomorphic characterization of Cu(II), Ni(II) and Pd(II) complexes with azomethine and chalcone as bridging group, Indian J. Chem. Sec. A 44A (2005) 265–270.
[58] D. Kilveson, Publications of Daniel Kivelson, J. Phy. Chem. B 101 (1997) 8631–8634.
[59] B.J. Hathaway, A.A.G. Tomlinson, The electronic properties and stereochemistry of mono-nuclear complexes of the copper(II) ion, Coord. Chem. Rev. 5 (1970) 143–207.
[60] A.J. Bard, L.R. Faulkner, Electrochemical Methods, second ed., Wiley, New York, 2001.
[61] S.A. Patil, S.N. Unki, D.K. Ajaykumar, H.N. Vinod, S.B. Prema, Co(II), Ni(II) and Cu(II) complexes with coumarin-8-yl Schiff-bases:spectroscopic, in vitro antimicrobial, DNA cleavage and fluorescence studies, Spectrochim. Acta Part A 79 (2011) 1128–1136.
[62] Z.H. Chohan, M. Arif, M.A. Akhtar, C.T. Supuran, Metal-based antibacterial and antifungal agents: synthesis, characterization, and *in vitro* biological evaluation of Co(II), Cu(II), Ni(II), and Zn(II) complexes with amino acid-derived compounds, Bioinorg. Chem. Appl. 2006 (2006) 1–14.
[63] K.N. Thimmaiah, W.D. Lioyd, G.T. Chandrappa, Stereochemistry and fungitoxicity of complexes of p-anisaldehydethiosemicarbazone with Mn(II), Fe(II), Co(II) and Ni(II), Inorg. Chim. Acta 106 (1985) 81–85.

[64] Z.H.A. Wahab, M.M. Mashaly, A.A. Salman, B.A. El-Shetary, A.A. Faheim, Co(II), Ce(III) and UO_2(VI) bis-salicylatothiosemicarbazide complexes: binary and ternary complexes, thermal studies and antimicrobial activity, Spectrochim. Acta Part A 60 (2004) 2861–2873.

[65] B.N. Meyer, N.R. Ferrigni, J.E. Putnam, L.B. Jacobsen, D.E. Nichols, J.L. McLaughlin, Brine shrimp: a convenient general bioassay for active plant constituents, Planta Med. 45 (5) (1982) 31–34.

[66] M.J. Waring., 1977. In: G.C.K. Roberts (Ed.), Drug Action at the Molecular Level, Macmillan, London 167.